

# Modeling Recurrent Safety-critical Events among Commercial Truck Drivers: A Bayesian Hierarchical Jump Power Law Process

Miao Cai

*Saint Louis University, Saint Louis, MO 63104*

Amir Mehdizadeh

*Auburn University, Auburn, AL 36849*

Qiong Hu

*Auburn University, Auburn, AL 36849*

Mohammad Ali Alamdar Yazdi

*Johns Hopkins University, Baltimore, MD 21202*

Alexander Vinel

*Auburn University, Auburn, AL 36849*

Fadel M. Megahed

*Miami University, Oxford, OH 45056*

Karen C. Davis

*Miami University, Oxford, OH 45056*

Hong Xian

*Saint Louis University, Saint Louis, MO 63104*

Steven E. Rigdon

*Saint Louis University, Saint Louis, MO 63104*

July 1, 2020

## Abstract

Many transportation safety studies aim to predict crashes based on aggregated road segment data. As an increasing number of naturalistic driving studies have been initiated in the recent decade, safety-critical events (SCEs) such as hard brakes are widely used as a proxy measure of driving risk. Different from real crashes, multiple SCEs can occur in a driving shift and they do not interrupt the state of driving. Motivated by a growing need of analyzing recurrent SCEs and the feature that multiple trips are nested within a shift for commercial truck drivers, we proposed a Bayesian hierarchical non-homogeneous Poisson process with power law process intensity function and an innovative Bayesian hierarchical jump power law process. We specified the parameterization, intensity functions, and likelihood functions for the two models and presented the estimation results for correctly and wrongly specified models based on simulated data. The two models are then applied to a naturalistic driving data of over 13 million driving records and 8,407 SCEs generated by 496 commercial truck drivers. Supplementary materials including simulated data and parameter estimation for reproducing the work, are available as an online supplement.

*Keywords:* trucking; safety-critical events; reliability; power law process

## 1. INTRODUCTION

Traditional trucking safety studies apply classification or count data models to predict the occurrence or number of crashes in certain road segments for a fixed amount of time based on policy reports data (Lord and Mannering, 2010; Savolainen et al., 2011; Mannering and Bhat, 2014). These retrospective crash prediction studies are inherently limited in the sample size of crashes, selection of control groups, and undercount of less severe crashes. Large-scale naturalistic driving studies that continuously record real-world driving data using unobtrusive instruments have recently been proposed as an innovative method for transportation safety research (Guo, 2019). Instead of studying real crashes, naturalistic driving studies use kinematic safety-critical events (SCEs) such as hard brakes as a proxy measure of driving risk. Although SCEs can still be analyzed using classification and count data models (Kim et al., 2013), these events are inherently different from crashes: there can be at most one crash in a working shift and the drivers have to stop once a crash occurs; in contrast, there can be multiple SCEs in a working shift and the drivers can continue driving even if SCEs occur.

Commercial truck drivers are on the road for an extended period of time and commonly face fatigue problems. Investigating the driving reliability using SCEs can contribute to understanding fatigue problems among commercial truck drivers and optimize route and shift scheduling. Previous studies tend to use traditional classification or count data models (Kim et al., 2013; Chen et al., 2016), or change-point models for naturalistic driving data sets (Chen and Guo, 2016; Li et al., 2017, 2018; Liu and Guo, 2019; Liu et al., 2019; Guo et al., 2019). These models are limited in two aspects. First, retrospective reports are

collecting crashes at road segments and non-crashes are selected randomly to match the crashes, which resembles a case-control study design. By comparison, naturalistic driving data sets follow the drivers or vehicles for a certain amount of time. Therefore, the sampling units in naturalistic driving data sets are drivers instead of road segments, which resembles a prospective cohort study design (Mehdizadeh et al., 2020). Since the same drivers tend to have similar driving patterns, it is logical to apply hierarchical models that account for driver-level effects to naturalistic driving data sets. Second, commercial truck drivers, especially long-haul truck drivers, must take at least one break in long-distance transporting as required by Federal Motor Carrier Safety Administration (2017). Researcher would assume that some level of fatigue alleviation and reliability change occur at these short breaks.

In consideration of these gaps, we first introduced a Bayesian hierarchical non-homogeneous Poisson process with the power law process (PLP) intensity function to model SCEs within shifts. This model accounts for driver-level unobserved heterogeneity by specifying driver-level random intercepts for the rate parameter in PLP. On the other hand, since the Federal Motor Carrier Safety Administration (2017) regulates that drivers who transports property and delivers materials must a) be on duty for no more than 14 hours; b) drive for no more than 11 hours, and c) take a at least 30-minute break by the eight hour of on duty, a property-carrying truck driver must have at least one break if they are on road for more than eight hours. To account for this feature of multiple trips and breaks nested within a shift among commercial truck drivers, we then propose a Bayesian hierarchical jump power law process (JPLP) to take potential reliability changes at the time of rests into consideration.

The structure of this article is as follows. In Section 2, we define our terminology and notation for shifts, trips, and events for naturalistic driving data generated by commercial

63 truck drivers. In Section 3, we specify our proposed PLP and JPLP models, their inten-  
64 sity functions and likelihood functions. In Section 4, simulation studies are conducted to  
65 demonstrate the validity of our code and the consequences if the models are not specified  
66 correctly. In section 5, we present the results of real data analyses for 496 commercial truck  
67 drivers using PLP and JPLP. Strengths, possible limitations, and future research directions  
68 are discussed in Section 6. A simulated data set, description on data structure, and Stan and  
69 R code for Bayesian PLP and JPLP estimation are provided in the supplementary material.

## 2. TERMINOLOGY AND NOTATION

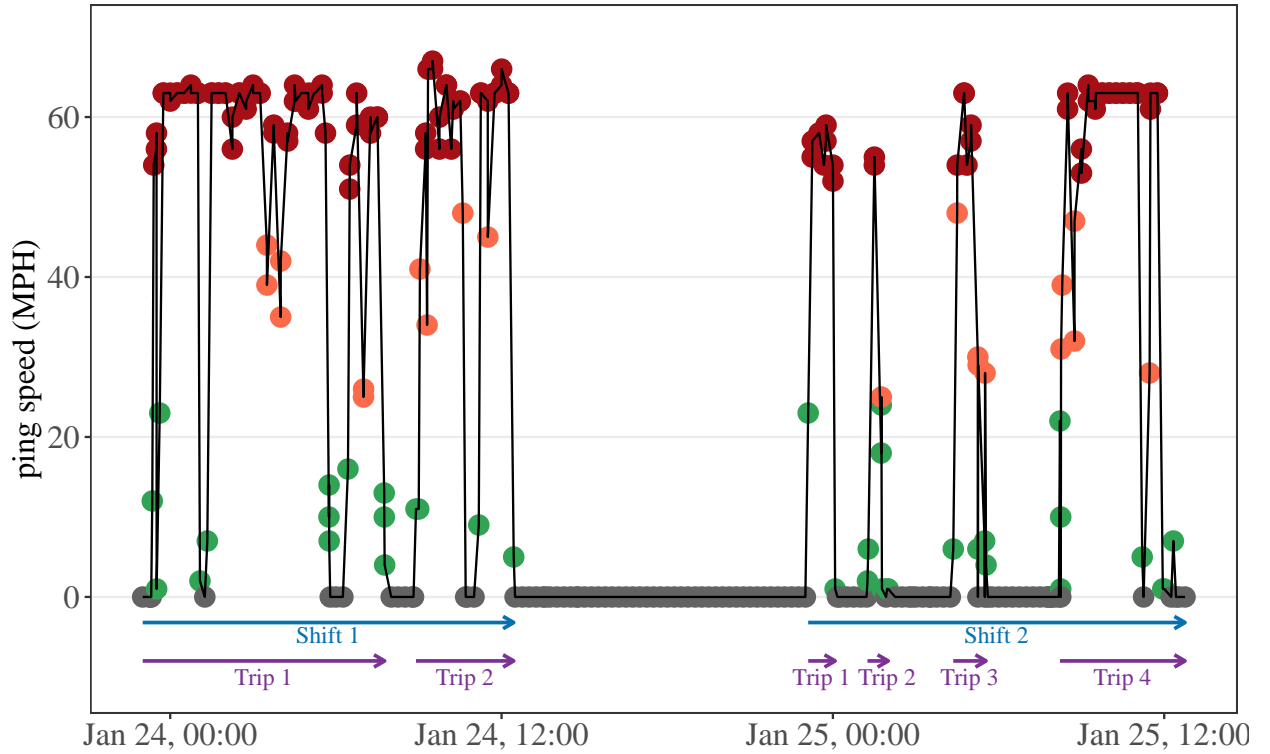


Figure 1: Naturalistic truck driving real-time ping data (points) and the aggregation process from pings to shifts and trips (arrows).

71 Figure 1 presents a time series plot of speed data for a sample truck driver (including two  
72 shifts and six trips nested within the shifts) and arrows suggesting shifts and trips. We use

73  $d = \{1, 2, \dots, D\}$  as the notation for different drivers. A shift  $s = \{1, 2, \dots, S_d\}$  is on-duty  
74 periods with no breaks longer than 10 hours for driver  $d$ . As the Federal Motor Carrier Safety  
75 Administration (2017) requires, a shift must be no more than 14 hours with no more than  
76 11 hours of driving, and this leads to the phenomena that multiple trips  $r = \{1, 2, \dots, R_{d,s}\}$   
77 are separated by breaks longer than 30 minutes but less than 10 hours for each driver  $d$  and  
78 shift  $s$ .

79 SCEs can occur any time in the trips whenever preset kinematic thresholds are trigger  
80 by the driver. We use  $i = \{1, 2, \dots, I_{d,s}\}$  as notations for the  $i$ -th SCE for driver  $d$  in shift  
81  $s$ . For each SCE,  $t_{d,s,i}$  is the time to the  $i$ -th SCE for driver  $d$  measured from the beginning  
82 of the  $s$ -shift and the rest times between trips are excluded from calculation.  $n_{d,s,r}$  is the  
83 number of SCEs for trip  $r$  within shift  $s$  for driver  $d$ .  $a_{d,s,r}$  is the end time of trip  $r$  within  
84 shift  $s$  for driver  $d$ .

### 85 3. MODELS

#### 86 3.1 Non-homogeneous Poisson Process (NHPP) and Power Law Process

We assume the time to a SCE  $t$  follows a non-homogeneous Poisson process, whose inten-  
sity function  $\lambda(t)$  is non-constant. The intensity function is assumed to have the following  
function form:

$$\lambda_{\text{PLP}}(t) = \beta \theta^{-\beta} t^{\beta-1}, \quad (1)$$

87 where the shape parameter  $\beta$  indicates reliability improvement ( $\beta < 1$ ), constant ( $\beta = 1$ ),  
88 or deterioration ( $\beta > 1$ ), and the scale parameter  $\theta$  determines the rate of events. Here  
89 we assume the intensity function of a power law process because it has a flexible functional

90 form, relatively simple statistical inference, and is a well-established model (Rigdon and  
 91 Basu, 1989, 2000).

### 92 3.2 Bayesian Hierarchical Power Law Process (PLP)

The Bayesian hierarchical power law process is parameterized as:

$$\begin{aligned}
 t_{d,s,1}, t_{d,s,2}, \dots, t_{d,s,n_{d,s}} &\sim \text{PLP}(\beta, \theta_{d,s}, \tau_{d,s}) \\
 \beta &\sim \text{Gamma}(1, 1) \\
 \log \theta_{d,s} &= \gamma_{0d} + \gamma_1 x_{d,s,1} + \gamma_2 x_{d,s,2} + \dots + \gamma_k x_{d,s,k} \\
 \gamma_{01}, \gamma_{02}, \dots, \gamma_{0D} &\sim \text{i.i.d. } N(\mu_0, \sigma_0^2) \\
 \gamma_1, \gamma_2, \dots, \gamma_k &\sim \text{i.i.d. } N(0, 10^2) \\
 \mu_0 &\sim N(0, 5^2) \\
 \sigma_0 &\sim \text{Gamma}(1, 1),
 \end{aligned} \tag{2}$$

where  $t_{d,s,i}$  is the time to the  $i$ -th event for driver  $d$  in shift  $s$ ,  $\tau_{d,s} = a_{d,s,R_{d,s}}$  is the length of time of shift  $s$  (truncation time) for driver  $d$ , and  $n_{d,s} = \sum_{r=1}^{n_{d,s}}$  is the number of SCEs in shift  $s$  for driver  $d$ . The likelihood function of event times generated from a PLP for driver  $d$  in shift  $s$  is given in Rigdon and Basu (2000, Section 2.3.2, Page 60):

$$\begin{aligned}
 L_{d,s}(\beta, \gamma_{0d}, \gamma | \mathbf{X}_d, \mathbf{W}_s) &= \left( \prod_{i=1}^{n_{d,s}} \lambda_{\text{PLP}}(t_{d,s,i}) \right) \exp\left(- \int_0^{\tau_{d,s}} \lambda_{\text{PLP}}(u) du\right) \\
 &= \begin{cases} \exp\left(- (\tau_{d,s}/\theta_{d,s})^\beta\right), & \text{if } n_{d,s} = 0, \\ \left( \prod_{i=1}^{n_{d,s}} \beta \theta_{d,s}^{-\beta} t_{d,s,i}^{\beta-1} \right) \exp\left(- (\tau_{d,s}/\theta_{d,s})^\beta\right), & \text{if } n_{d,s} > 0, \end{cases} \tag{3}
 \end{aligned}$$

where  $\mathbf{X}_d$  indicates driver specific variables (e.g. driver age and gender),  $\mathbf{W}_s$  represents shift specific variables (e.g. precipitation and traffic), and  $\theta_{d,s}$  is the function of parameters  $\gamma_{0d}, \gamma_1, \gamma_2, \dots, \gamma_k$  and variables  $x_{d,s,1}, x_{d,s,2}, \dots, x_{d,s,k}$  given in the third line of Equation 2. The full likelihood function for all drivers are:

$$L = \prod_{d=1}^D \prod_{s=1}^{S_d} L_{d,s}(\beta, \gamma_{0d}, \gamma | \mathbf{X}_d, \mathbf{W}_s) \quad (4)$$

93 where  $L_{d,s}(\beta, \gamma_{0d}, \gamma | \mathbf{X}_d, \mathbf{W}_s)$  is given in Equation 3.

### 94 3.3 Bayesian Hierarchical Jump Power Law Process (JPLP)

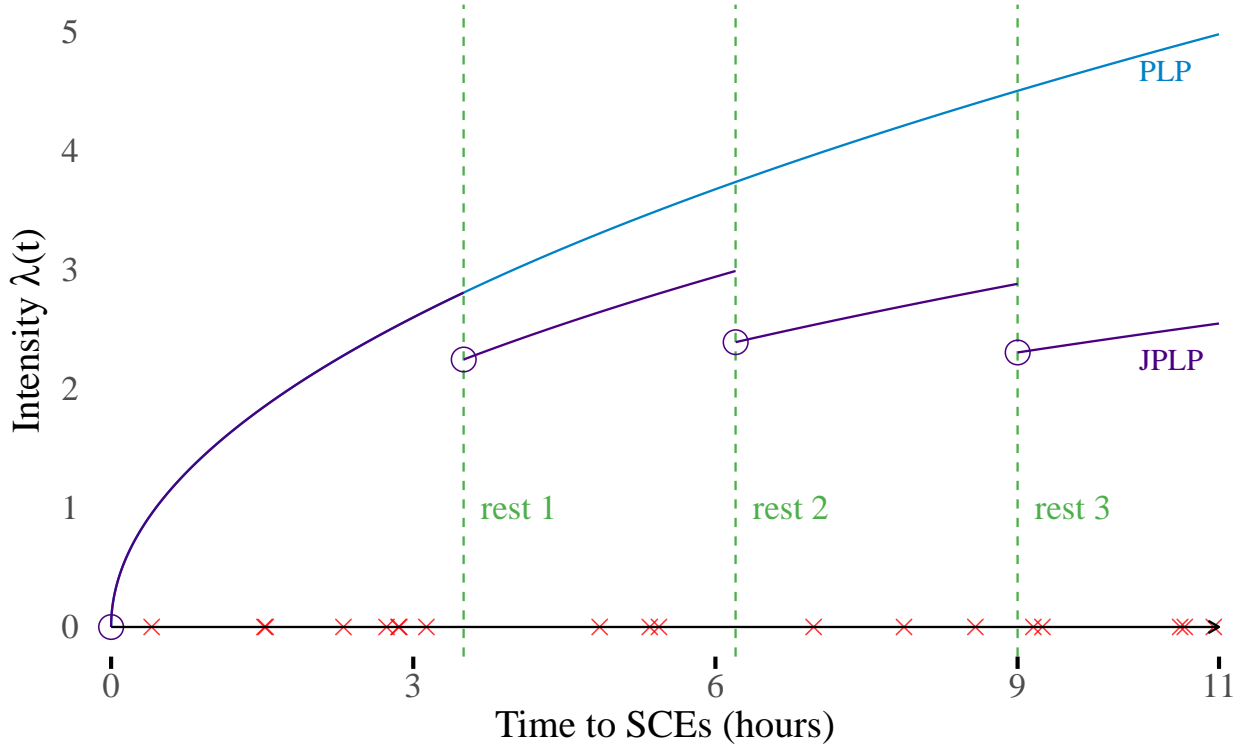


Figure 2: Simulated intensity function of PLP and JPLP. The  $x$ -axis shows time in hours since start and  $y$ -axis shows the intensity of SCEs. The crosses mark the time to SCEs and the vertical dotted lines indicates the time of the rests. Parameters for this simulated data set: shape parameters  $\beta = 1.2$ , rate parameter  $\theta = 2$ , jump parameter  $\kappa = 0.8$ .



95 Since the Bayesian hierarchical PLP in Subsection 3.2 does not account for the rests  
 96 ( $r = \{1, 2, \dots, R_{d,s}\}$ ) within shifts and associated potential reliability improvement. In this  
 97 subsection, we propose a Bayesian hierarchical JPLP with an additional jump parameter  $\kappa$ .  
 98 Figure 2 presents the intensity functions of PLP and JPLP. The intensity function of PLP  
 99 is a smooth curve with concave-down trend when  $\beta > 1$  (the first segment of the two curves  
 100 overlaps), while the JPLP has a piecewise appearance. Whenever the driver takes a break,  
 101 the intensity function of a JPLP jump by a certain amount  $\kappa$ .

Our proposed JPLP has the following piecewise intensity function:

$$\begin{aligned}
 \lambda_{\text{JPLP}}(t|d, s, r, \beta, \gamma_{0d}, \gamma, \mathbf{X}_d, \mathbf{W}_s) = & \\
 & \left\{ \begin{array}{ll} \kappa^0 \lambda(t|\beta, \gamma_{0d}, \gamma, \mathbf{X}_d, \mathbf{W}_s), & 0 < t \leq a_{d,s,1}, \\ \kappa^1 \lambda(t|\beta, \gamma_{0d}, \gamma, \mathbf{X}_d, \mathbf{W}_s), & a_{d,s,1} < t \leq a_{d,s,2}, \\ \dots & \dots \\ \kappa^{R-1} \lambda(t|\beta, \gamma_{0d}, \gamma, \mathbf{X}_d, \mathbf{W}_s), & a_{d,s,R-1} < t \leq a_{d,s,R}, \end{array} \right. \quad (5) \\
 & = \kappa^{r-1} \lambda(t|d, s, r, \kappa, \beta, \gamma_{0d}, \gamma, \mathbf{X}_d, \mathbf{W}_s), \quad a_{d,s,r-1} < t \leq a_{d,s,r},
 \end{aligned}$$

102 where the introduced parameter  $\kappa$  is the amount of intensity function change once the driver  
 103 takes a break, and  $a_{d,s,r}$  is the end time of trip  $r$  within shift  $s$  for driver  $d$ . By definition,  
 104 the end time of the 0-th trip  $a_{d,s,0} = 0$ , and the end time of the last trip for the  $d$ -driver  
 105 within the  $s$ -th shift  $a_{d,s,R_{d,s}}$  equals the shift end time  $\tau_{d,s}$ . We assume that this  $\kappa$  is constant  
 106 across drivers and shifts.

The Bayesian hierarchical JPLP model is parameterized as:

$$\begin{aligned}
t_{d,s,1}, t_{d,s,2}, \dots, t_{d,s,n_{d,s}} &\sim \text{JPLP}(\beta, \theta_{d,s}, \tau_{d,s}, \kappa) \\
\beta &\sim \text{Gamma}(1, 1) \\
\log \theta_{d,s} &= \gamma_{0d} + \gamma_1 x_{d,s,1} + \gamma_2 x_{d,s,2} + \dots + \gamma_k x_{d,s,k} \\
\kappa &\sim \text{Uniform}(0, 2) \\
\gamma_{01}, \gamma_{02}, \dots, \gamma_{0D} &\sim \text{i.i.d. } N(\mu_0, \sigma_0^2) \\
\gamma_1, \gamma_2, \dots, \gamma_k &\sim \text{i.i.d. } N(0, 10^2) \\
\mu_0 &\sim N(0, 5^2) \\
\sigma_0 &\sim \text{Gamma}(1, 1),
\end{aligned} \tag{6}$$

The notations are identical with those in Equation 2 except for the extra  $\kappa$  parameter. Here we set the prior distribution for  $\kappa$  as  $\text{uniform}(0, 2)$ , which is assuming that the intensity function can jump down to 0 or increase by up to 100% at the time of rests. Similarly, the likelihood function of event times generated from a JPLP for driver  $d$  on shift  $s$  is:

$$\begin{aligned}
L_{d,s}^*(\kappa, \beta, \gamma_{0d}, \gamma | \mathbf{X}_d, \mathbf{W}_s) &= \left( \prod_{i=1}^{n_{d,s}} \lambda_{\text{JPLP}}(t_{d,s,i}) \right) \exp\left(-\int_0^{\tau_{d,s}} \lambda_{\text{JPLP}}(u) du\right) \\
&\begin{cases} \exp\left(-\int_0^{\tau_{d,s}} \lambda_{\text{JPLP}}(u) du\right), & \text{if } n_{d,s} = 0, \\ \left(\prod_{i=1}^{n_{d,s}} \lambda_{\text{JPLP}}(t_{d,s,i})\right) \exp\left(-\int_0^{\tau_{d,s}} \lambda_{\text{JPLP}}(u) du\right), & \text{if } n_{d,s} > 0, \end{cases} \tag{7}
\end{aligned}$$

107 where the piecewise intensity function  $\lambda_{\text{JPLP}}(t_{d,s,i})$  is given in Equation 5.

However, since the intensity function depends on the trip  $r$  for the same driver  $d$  on

shift  $s$ , it is hard to write out the specific form of Equation 7. Instead, we can rewrite the likelihood function at trip level, where the intensity function  $\lambda_{\text{JPLP}}$  is fixed for driver  $d$  on shift  $s$  and trip  $r$ :

$$L_{d,s,r}^*(\kappa, \beta, \gamma_{0d}, \gamma | \mathbf{X}_d, \mathbf{W}_r) = \begin{cases} \exp \left( - \int_{a_{d,s,r-1}}^{a_{d,s,r}} \lambda_{\text{JPLP}}(u) du \right), & \text{if } n_{d,s,r} = 0, \\ \left( \prod_{i=1}^{n_{d,s,r}} \lambda_{\text{JPLP}}(t_{d,s,r,i}) \right) \exp \left( - \int_{a_{d,s,r-1}}^{a_{d,s,r}} \lambda_{\text{JPLP}}(u) du \right), & \text{if } n_{d,s,r} > 0, \end{cases} \quad (8)$$

where  $t_{d,s,r,i}$  is the time to the  $i$ -th SCE for driver  $d$  on shift  $s$  and trip  $r$  measured from the beginning of the shift,  $n_{d,s,r}$  is the number of SCEs for driver  $d$  on shift  $s$  and trip  $r$ . Compared to the PLP likelihood function given in Equation 4 where  $\mathbf{W}_s$  are assumed to be fixed numbers during an entire shift, the rewritten likelihood function for JPLP in Equation 8 assumes external covariates  $\mathbf{W}_r$  vary between different trips in a shift. In this way, JPLP can account for the variability between different trips within a shift.

Therefore, the overall likelihood function for drivers  $d = 1, 2, \dots, D$ , their corresponding shifts  $s = \{1, 2, \dots, S_d\}$ , and trips  $r = \{1, 2, \dots, R_{d,s}\}$  is:

$$L^* = \prod_{d=1}^D \prod_{s=1}^{S_d} \prod_{r=1}^{R_{d,s}} L_{d,s,r}^* \quad (9)$$

where  $L_{d,s,r}^*$  is a likelihood function given in Equation 8, in which the intensity function  $\lambda_{\text{JPLP}}$  has a fixed functional form provided in the last line of Equation 5 for a certain driver  $d$  in a given shift  $s$  and trip  $r$ .

## 4. SIMULATION STUDY

### 4.1 Simulation setting

We conducted a simulation study to evaluate the performance of our proposed NHPP and JPLP under different simulation scenarios. We performed 1,000 simulations to each of the following three scenarios with different number of drivers  $D = \{10, 25, 50, 75, 100\}$ :

1. Data generated from a PLP and estimated assuming a PLP (PLP),
2. Data generated from a JPLP, but estimated assuming a PLP (JPLP),
3. Data generated from a JPLP and estimated assuming a JPLP ( $\text{PLP} \leftarrow \text{JPLP}$ ).

The scenario “data generated from a PLP, but estimated assuming a JPLP” is not considered here since it is not theoretically possible: if the data is generated from a NHPP with PLP intensity function, then there are no breaks within shifts and it is pointless to estimate the data assuming a JPLP.

Specifically, for each driver, the number of shifts is simulated from a Poisson distribution with the mean parameter of 10. We assume there are three predictor variables  $x_1, x_2, x_3$  for  $\theta$  ( $k = 3$ ).  $x_1, x_2, x_3$  and the shift time  $\tau_{d,s}$  are generated from the following process:

$$\begin{aligned}
 x_1 &\sim \text{Normal}(1, 1^2) \\
 x_2 &\sim \text{Gamma}(1, 1) \\
 x_3 &\sim \text{Poisson}(2) \\
 \tau_{d,s} &\sim \text{Normal}(10, 1.3^2)
 \end{aligned} \tag{10}$$

The parameters and hyperparameters are assigned the following values or generated from

the following process:

$$\begin{aligned}
\mu_0 &= 0.2, \sigma_0 = 0.5, \\
\gamma_{01}, \gamma_{02}, \dots, \gamma_{0D} &\sim \text{i.i.d. } N(\mu_0, \sigma_0^2) \\
\gamma_1 &= 1, \gamma_2 = 0.3, \gamma_3 = 0.2 \\
\theta_{d,s} &= \exp(\gamma_{0d} + \gamma_1 x_1 + \gamma_2 x_2 + \gamma_3 x_3) \\
\beta &= 1.2, \kappa = 0.8.
\end{aligned} \tag{11}$$

After the predictor variables, shift time, and parameters are generated, the time to events

$t_{d,s,1}, t_{d,s,2}, \dots, t_{d,s,n_{d,s}}$  and  $t_{d,s,1}^*, t_{d,s,2}^*, \dots, t_{d,s,n_{d,s}}^*$  are generated from PLP and JPLP:

$$\begin{aligned}
t_{d,s,1}, t_{d,s,2}, \dots, t_{d,s,n_{d,s}} &\sim \text{PLP}(\beta, \theta_{d,s}, \tau_{d,s}) \\
t_{d,s,1}^*, t_{d,s,2}^*, \dots, t_{d,s,n_{d,s}}^* &\sim \text{JPLP}(\beta, \theta_{d,s}, \tau_{d,s}, \kappa)
\end{aligned} \tag{12}$$

The parameters are then estimated using the likelihood functions given in Equation 4 and 9 using the probabilistic programming language **Stan** in R (Carpenter et al., 2017; Stan Development Team, 2018), which uses efficient Hamiltonian Monte Carlo to sample from the posterior distributions. For each simulation, one chain is applied, with 2,000 warmup and 2,000 post-warmup iterations drawn from the posterior distributions.

## 4.2 Simulation results

The simulation results are shown in Table 1. For the five sets of drivers  $D = \{10, 25, 50, 75, 100\}$  in each of the three scenarios, the mean of posterior mean estimates, mean of estimation bias  $\Delta = |\hat{\mu} - \mu|$ , and mean of standard error estimates for parameters  $\beta, \kappa, \gamma_1, \gamma_2, \gamma_3$  and

hyperparameters  $\mu_0$  and  $\sigma$  are calculated.

Table 1: Simulation results for PLP, JPLP, and PLP  $\leftarrow$  JPLP

sim_scaio	D	estimate	$\gamma_1$	$\gamma_2$	$\gamma_3$	$\beta$	$\kappa$	$\mu_0$	$\sigma_0$
PLP	10	bias $\Delta$	0.0203	0.0095	0.0067	0.0102		0.0282	0.0527
PLP	25	bias $\Delta$	0.0066	0.0046	0.0012	0.0045		0.0015	0.0220
PLP	50	bias $\Delta$	0.0040	0.0033	0.0005	0.0017		0.0068	0.0077
PLP	75	bias $\Delta$	0.0034	0.0004	0.0007	0.0017		0.0026	0.0091
PLP	100	bias $\Delta$	0.0009	0.0009	0.0003	0.0006		0.0034	0.0042
PLP	10	s.e.	0.0777	0.0696	0.0413	0.0589		0.2401	0.1722
PLP	25	s.e.	0.0459	0.0414	0.0247	0.0360		0.1392	0.0916
PLP	50	s.e.	0.0316	0.0286	0.0172	0.0254		0.0960	0.0610
PLP	75	s.e.	0.0258	0.0232	0.0139	0.0207		0.0784	0.0497
PLP	100	s.e.	0.0220	0.0198	0.0119	0.0179		0.0667	0.0420
JPLP	10	bias $\Delta$	0.0331	0.0218	0.0092	0.0226	0.0149	0.0401	0.0696
JPLP	25	bias $\Delta$	0.0158	0.0081	0.0039	0.0131	0.0084	0.0202	0.0219
JPLP	50	bias $\Delta$	0.0037	0.0012	0.0039	0.0057	0.0032	0.0014	0.0111
JPLP	75	bias $\Delta$	0.0060	0.0012	0.0006	0.0058	0.0028	0.0057	0.0097
JPLP	100	bias $\Delta$	0.0048	0.0003	0.0008	0.0043	0.0023	0.0004	0.0041
JPLP	10	s.e.	0.0992	0.0834	0.0498	0.0828	0.0573	0.2556	0.1854
JPLP	25	s.e.	0.0586	0.0477	0.0288	0.0512	0.0360	0.1453	0.0960
JPLP	50	s.e.	0.0406	0.0334	0.0201	0.0366	0.0256	0.0999	0.0647
JPLP	75	s.e.	0.0331	0.0272	0.0164	0.0298	0.0208	0.0812	0.0519
JPLP	100	s.e.	0.0287	0.0233	0.0141	0.0258	0.0179	0.0699	0.0442
PLP $\leftarrow$ JPLP	10	bias $\Delta$	0.1923	0.0645	0.0434	0.1843		0.1234	0.1599
PLP $\leftarrow$ JPLP	25	bias $\Delta$	0.1769	0.0514	0.0374	0.1740		0.0866	0.1053
PLP $\leftarrow$ JPLP	50	bias $\Delta$	0.1718	0.0531	0.0355	0.1734		0.0854	0.0977
PLP $\leftarrow$ JPLP	75	bias $\Delta$	0.1686	0.0511	0.0346	0.1724		0.0874	0.0960
PLP $\leftarrow$ JPLP	100	bias $\Delta$	0.1674	0.0512	0.0349	0.1713		0.0811	0.0925
PLP $\leftarrow$ JPLP	10	s.e.	0.1041	0.0946	0.0559	0.0580		0.2952	0.2078
PLP $\leftarrow$ JPLP	25	s.e.	0.0609	0.0546	0.0329	0.0354		0.1671	0.1095
PLP $\leftarrow$ JPLP	50	s.e.	0.0423	0.0383	0.0230	0.0250		0.1167	0.0743
PLP $\leftarrow$ JPLP	75	s.e.	0.0344	0.0310	0.0186	0.0204		0.0946	0.0601
PLP $\leftarrow$ JPLP	100	s.e.	0.0297	0.0266	0.0160	0.0177		0.0810	0.0514

When the models were specified correctly, the biases converges to 0 as the number of drivers increases; the standard errors converges to 0 roughly proportional to the square root of the number of drivers ( $\sqrt{D}$ ), which is consistent with the central limit theorem. When the models are not specified correctly, there are still a fair amount of biases when the number

of drivers increases and the speed of converging to zero is not consistent with either the other two correctly specified simulation scenarios or the central limit theorem. The Gelman-Rubin diagnostic  $\hat{R}$  were all lower than 1.1 and no low effective sample size (ESS) issues were reported in **Stan**, suggesting that steady posterior distributions were reached while estimating for the simulated data sets.

## 5. REAL DATA ANALYSIS

### 5.1 Data description

A naturalistic truck driving data set was provided to the research team by a national commercial trucking company in North America. The data set includes 496 regional drivers who move freights in regional routes that may include several surrounding states. A total of 13,187,289 ping records were generated between April 2015 and March 2016, with a total traveled distance of 20,042,519 miles in 465,641 hours (average speed 43 miles per hour). Each ping records the date and time (year, month, day, hour, minute, and second), latitude and longitude (specific to five decimal places), driver identification number, and speed at that time point. These pings were then aggregated into 64,860 shifts and 180,408 trips.

On the other hand, 8,407 kinematic SCEs were recorded independent of the pings, including 3941 (46.9%) headway, 3576 (42.5%) hard brakes, 869 (10.3%) collision mitigation, and 21 (0.2%) rolling stability. Historic weather data, including precipitation probability, precipitation intensity, and wind speed, were queried from the **DarkSky** Application Programming Interface, which provides historic real-time and hour-by-hour nationwide historic weather conditions for specific latitude-longitude-date-time combinations (The Dark Sky Company, LLC, 2020). The weather data were then merged back to pings data and aggregated to shift-

and trip-level by taking the mean.

## 5.2 Real data analysis results

We applied the hierarchical Bayesian PLP and JPLP models to this data as specified in Equations 2 and 6. Since we have four types of SCEs, we then applied the JPLP to the four different types of SCEs separately. Collision mitigation and rolling stability were combined as one type because the later one is very scare and will yield very unstable estimates if modeled alone. Samples of the posterior distributions were drawn using the probabilistic programming language **Stan** in R (Carpenter et al., 2017; Stan Development Team, 2018). The convergence of Hamiltonian Monte Carlo was checked using Gelman-Rubin diagnostic statistics  $\hat{R}$  (Gelman et al., 1992), effective sample size (ESS), and trace plots.

Table 2 presents the posterior mean, 95% credible interval (CI), Gelman-Rubin diagnostic statistics  $\hat{R}$ , and ESS for the sample 496 regional drivers using PLP and JPLP. In both the PLP and JPLP models, the posterior means of the shape parameters  $\beta$  are less than one and the 95% credible intervals exclude one, indicating SCEs occur in the early stages of the shifts. In JPLP, the reliability jump parameter  $\kappa$  was close to 1, suggesting that within-shift rests have very minor effects on the reliability of SCEs. Figure 3 shows the random intercepts  $\gamma_{0d}$  in both the PLP and JPLP present a fair amount of variability across different drivers. Besides, the random intercepts  $\gamma_{0d}$  are on average larger in JPLP than those in PLP models, while variability of random intercepts is similar in the two models. These patterns are consistent with the parameter estimates of  $\mu_0$  and  $\sigma_0$  in Table 2. All the Gelman-Rubin diagnostic statistics  $\hat{R}$  are less than 1.1 and the ESSs are greater than 1,000. The trace plots of important variables in the Appendix figure 4 indicate that all four chains for



the parameters are well mixed. All these evidence suggests that a steady state posterior distribution have been reached for the two models.

Table 2: Posterior mean, 95% credible interval, Rhat, and effective sample size (ESS) of PLP and JPLP models for 496 commercial truck drivers

Parameters	Power law process				Jump power law process			
	mean	95% CI	$\hat{R}$	ESS	mean	95% CI	$\hat{R}$	ESS
$\beta$	0.968	( 0.948, 0.988)	1.000	6,500	0.962	( 0.940, 0.985)	1.001	3,798
$\kappa$					1.020	( 0.995, 1.045)	1.000	5,400
$\mu_0$	3.038	( 2.397, 3.688)	1.001	2,979	3.490	( 2.899, 4.091)	1.001	3,079
$\sigma_0$	0.974	( 0.897, 1.058)	1.000	9,581	0.982	( 0.905, 1.066)	1.000	9,050
Age	0.003	(-0.005, 0.012)	1.001	2,250	0.004	(-0.005, 0.012)	1.001	2,566
Race: black	-0.113	(-0.329, 0.103)	1.002	1,951	-0.130	(-0.342, 0.087)	1.001	2,277
Race: other	-0.343	(-0.707, 0.021)	1.001	2,833	-0.361	(-0.729, 0.010)	1.001	3,334
Gender: female	-0.071	(-0.441, 0.300)	1.001	3,069	-0.071	(-0.435, 0.296)	1.001	4,162
Mean speed	0.019	( 0.016, 0.023)	1.000	20,229	0.015	( 0.013, 0.018)	1.000	19,827
Speed variation	0.026	( 0.017, 0.034)	1.000	24,825	0.017	( 0.013, 0.022)	1.000	13,127
Preci. intensity	-3.608	(-6.181, -0.935)	1.000	22,025	-2.136	(-3.785, -0.368)	1.000	24,397
Preci. prob.	0.397	( 0.168, 0.628)	1.000	21,416	0.121	(-0.050, 0.296)	1.000	25,329
Wind speed	0.018	( 0.008, 0.029)	1.000	32,980	0.010	( 0.001, 0.018)	1.000	33,093

95% CI: 95% credible interval; ESS: effective sample size;

PLP: power law process; JPLP: jump power law process;

Preci. intensity: precipitation intensity; Precip. prob.: precipitation probability.

We further estimated the JPLP models for different types of SCEs (headway, hard brakes, and collision mitigation and rolling stability), and the results are presented in Table 3. Headway and hard brake are similar: they have very close posterior mean and 95% credible intervals for parameters  $\beta$  and  $\kappa$ , although the hyperparameters for random intercepts are quite different. The results that  $\beta < 1$  and  $\kappa > 1$  suggest that headway and hard brake tend to occur in the early stages of driving shifts, and taking short breaks will slightly increase the intensity of these two events. In contrast, collision mitigation and rolling stability show a different pattern: they tend to occur in later stages of driving shifts, and taking short breaks

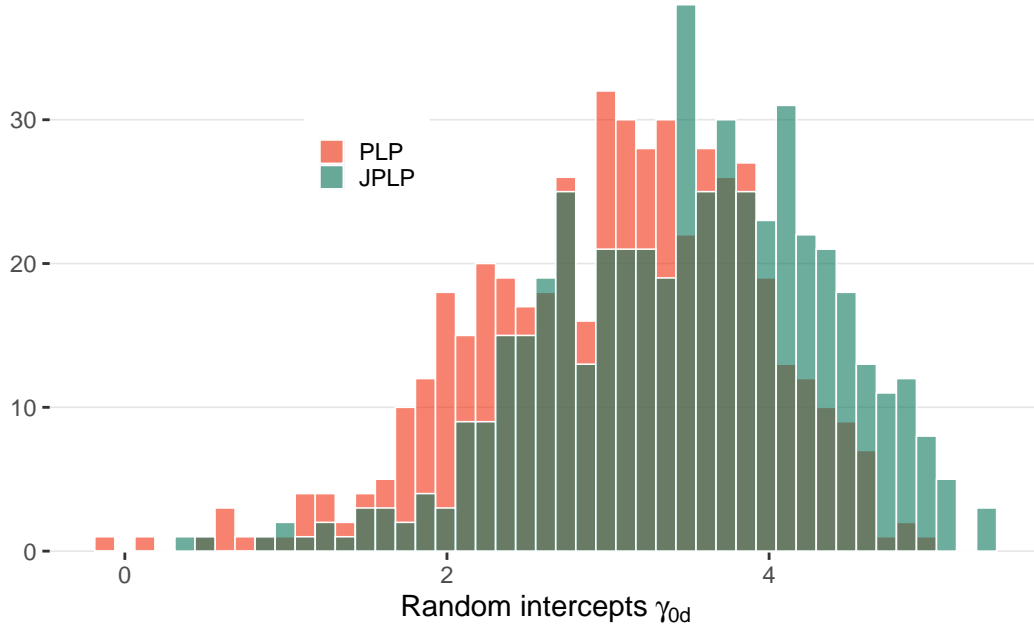


Figure 3: Histogram of random intercepts  $\gamma_{0d}$  across the 496 drivers.

will reduce the intensity of the event. The variability across drivers  $\sigma_0$  is more evidence for headway than hard brake, collision mitigation and rolling stability.

## 6. DISCUSSION

In this article, we proposed a Bayesian hierarchical NHPP with PLP intensity function and an innovative Bayesian hierarchical JPLP to model naturalistic truck driving data. Our motivation comes from more popular use of naturalistic driving data sets in the recent decade and real-life truck driving characteristics of multiple trips nested within shifts. The proposed JPLP accounts for the characteristics of multiple rests within a shift among commercial truck drivers. The intensity functions, parameterization forms, and likelihood functions are specified separately. Simulation studies showed the consistency of the Bayesian hierarchical estimation if the models are specified correctly, as well as the persistent bias when the models are not specified correctly. A case study of 496 commercial truck drivers demonstrates a fair

Table 3: Parameter estimates and 95% credible intervals for jump power law process on 496 truck drivers, stratified by different types of safety-critical events

Parameters	Headway	Hard brake	Collision mitigation & Rolling stability
$\beta$	0.989 ( 0.956, 1.023)	0.922 ( 0.889, 0.955)	1.020 ( 0.950, 1.096)
$\kappa$	1.034 ( 0.998, 1.071)	1.034 ( 0.996, 1.072)	0.890 ( 0.821, 0.964)
$\mu_0$	7.096 ( 6.083, 8.139)	3.470 ( 2.770, 4.199)	4.729 ( 3.836, 5.666)
$\sigma_0$	1.564 ( 1.411, 1.730)	1.073 ( 0.973, 1.182)	0.922 ( 0.786, 1.074)
Age	-0.006 (-0.020, 0.009)	0.011 ( 0.001, 0.021)	0.002 (-0.009, 0.012)
Race: black	0.184 (-0.170, 0.546)	-0.312 (-0.565, -0.064)	0.113 (-0.153, 0.386)
Race: other	0.306 (-0.340, 0.967)	-0.539 (-0.968, -0.106)	0.100 (-0.373, 0.605)
Gender: female	0.266 (-0.343, 0.870)	-0.217 (-0.654, 0.230)	-0.181 (-0.675, 0.309)
Mean speed	-0.026 (-0.031, -0.021)	0.043 ( 0.039, 0.047)	0.039 ( 0.032, 0.046)
Speed variation	-0.009 (-0.017, -0.002)	0.017 ( 0.010, 0.024)	0.013 (-0.002, 0.027)
Preci. intensity	-0.771 (-4.306, 3.188)	-1.912 (-3.924, 0.269)	-0.676 (-6.329, 6.297)
Preci. prob.	0.694 ( 0.376, 1.015)	-0.495 (-0.724, -0.263)	0.808 ( 0.206, 1.423)
Wind speed	0.003 (-0.009, 0.015)	0.019 ( 0.005, 0.034)	0.000 (-0.025, 0.026)

Preci. intensity: precipitation intensity; Precip. prob.: precipitation probability.

amount of variability exist across drivers. Headway and hard brake tend to occur in early stages while collision mitigation and rolling stability tend to occur in later stages.

The SCEs generated from naturalistic truck driving data are different from previous reliability problems and models in two aspects. Most previous studies either assume minimal repair or perfect repair (also known as renewal process). A minimal repair assumes the unit after the repair is exactly the same as it is before the repair (for example, our first proposed NHPP with a PLP intensity function), while a perfect repair assumes the unit is a completely new unit after repair (Rigdon and Basu, 2000). In the scenario of truck driving, although it is reasonable to assume that the drivers experience a perfect repair when they take a break of longer than 10 hours, researchers would not expect the reliability to be either perfectly

219 repaired or minimally repaired during a short break of around half an hour. Instead, a partial  
220 repair is a more proper assumption here.

221 On the other hand, even though some studies proposed partial repair reliability models  
222 such as the modulated PLP (Lakey and Rigdon, 1993; Black and Rigdon, 1996), none of these  
223 previously proposed models fit for the data here since the repairs are independent of the SCEs  
224 in naturalistic driving data. These previous models are based on high-tech devices such as  
225 aircraft manufacturing, which need immediate repair once a failure is detected. However in  
226 the case of naturalistic truck driving data sets, SCEs such as hard brakes and headway do  
227 not seriously influence the driving and drivers generally will keep driving even if SCEs occur.  
228 The repair (breaks) can be considered as independent of SCEs in our study. Although our  
229 case study is based on naturalistic truck driving data sets, the JPLP can applied to any type  
230 of drivers who drive for a long distance with at least one break.

231 Our work can be extended in several aspects in the future. First, the assumption of pro-  
232 portion reliability jump may not hold. Other proper assumptions include reliability jumping  
233 for a fixed-amount jump or jumping dependent on the length of the rest. Additionally, in our  
234 proposed JPLP, the length of breaks within shifts are ignored to simplify the parameterization  
235 and likelihood function. In truck transportation practice, longer breaks certainly have larger  
236 effects on reliability jump, hence the relationship between reliability jump and the length of  
237 breaks can have more complex functional forms, so it would be of interest to test different  
238 forms of reliability change as a function of the length of break.

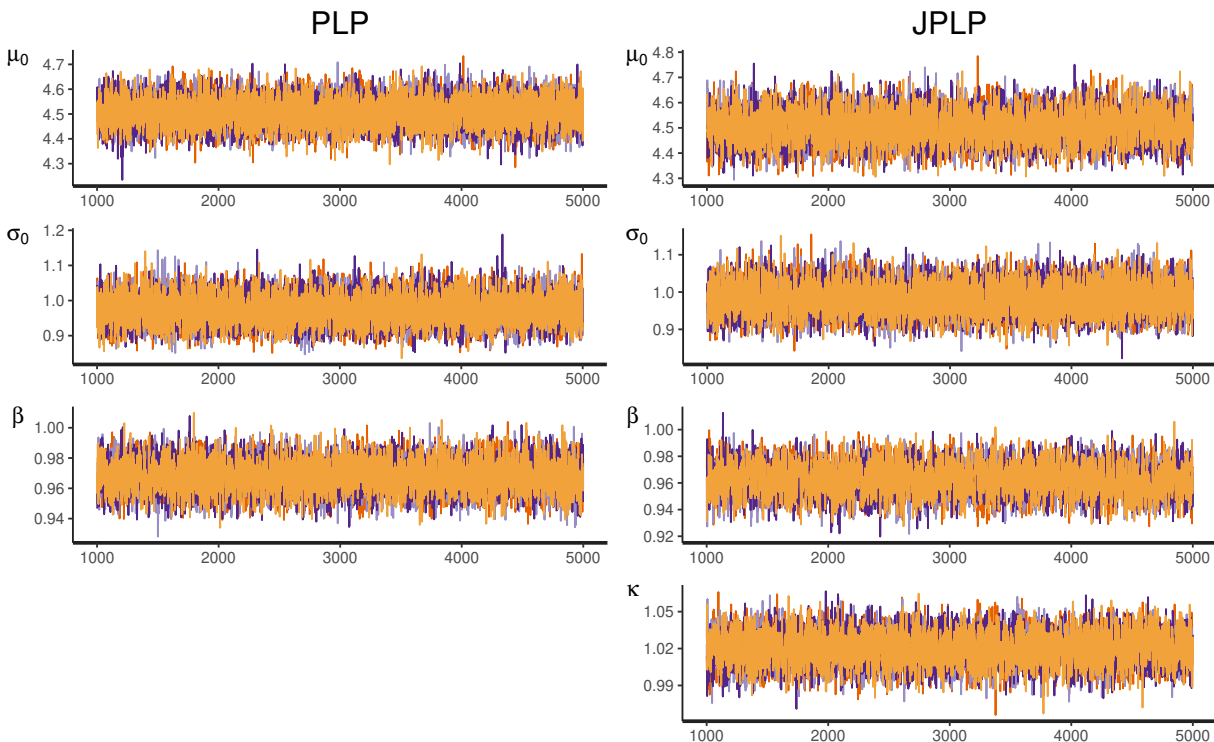


Figure 4: Trace plots of select parameters in PLP (left column) and JPLP (right column) for all types of SCEs

## SUPPLEMENTARY MATERIALS

Since the real truck driving data provided by our industry partner are confidential and cannot be made publicly accessible, we provided a simulated data set that is similar to our real data in data structure but has fewer drivers to be completed within a reasonable amount of time. The online supplementary materials contain the R code to simulate PLP and JPLP data, explanation on the data structure, and Stan and R code for Bayesian hierarchical PLP and JPLP estimation. The supplementary materials can be access at [https://github.com/caimiao0714/JPLP\\_sim](https://github.com/caimiao0714/JPLP_sim).

## ACKNOWLEDGEMENTS

The authors are grateful to our industry partner for providing us the naturalistic truck driving data for research in this study.

## FUNDING

The work was supported by the National Science Foundation (CMMI-1635927 and CMMI-1634992), the Ohio Supercomputer Center (PMIU0138 and PMIU0162). We also thank the DarkSky company for providing us five million free calls to their historic weather API.

## REFERENCES

- Black, S. E. and Rigdon, S. E. (1996). Statistical inference for a modulated power law process. *Journal of Quality Technology*, 28(1):81–90.
- Carpenter, B., Gelman, A., Hoffman, M. D., Lee, D., Goodrich, B., Betancourt, M., Brubaker, M., Guo, J., Li, P., and Riddell, A. (2017). Stan: A probabilistic programming language. *Journal of Statistical Software*, 76(1).
- Chen, C. and Guo, F. (2016). Evaluating the Influence of Crashes on Driving Risk Using Recent Event Models and Naturalistic Driving Study Data. *Journal of Applied Statistics*, 43(12):2225–2238.
- Chen, G. X., Fang, Y., Guo, F., and Hanowski, R. J. (2016). The influence of daily sleep patterns of commercial truck drivers on driving performance. *Accident analysis & prevention*, 91:55–63.

267 Federal Motor Carrier Safety Administration (2017). Summary of hours of service regula-  
268 tions. [Online; accessed 20-February-2019].

269 Gelman, A., Rubin, D. B., et al. (1992). Inference from iterative simulation using multiple  
270 sequences. *Statistical Science*, 7(4):457–472.

271 Guo, F. (2019). Statistical Methods for Naturalistic Driving Studies. *Annual Review of*  
272 *Statistics and Its Application*, 6:309–328.

273 Guo, F., Kim, I., and Klauer, S. G. (2019). Semiparametric Bayesian Models for Evaluating  
274 Time-Variant Driving Risk Factors Using Naturalistic Driving Data and Case-Crossover  
275 Approach. *Statistics in Medicine*, 38(2):160–174.

276 Kim, S., Chen, Z., Zhang, Z., Simons-Morton, B. G., and Albert, P. S. (2013). Bayesian Hi-  
277 erarchical Poisson Regression Models: An Application to a Driving Study With Kinematic  
278 Events. *Journal of the American Statistical Association*, 108(502):494–503.

279 Lakey, M. J. and Rigdon, S. E. (1993). Reliability Improvement Using Experimental De-  
280 sign. In *Annual Quality Congress Transactions-American Society for Quality Control*,  
281 volume 47, pages 824–824. American Society for Quality Control.

282 Li, Q., Guo, F., Kim, I., Klauer, S. G., and Simons-Morton, B. G. (2018). A Bayesian Finite  
283 Mixture Change-Point Model for Assessing the Risk of Novice Teenage Drivers. *Journal*  
284 *of Applied Statistics*, 45(4):604–625.

285 Li, Q., Guo, F., Klauer, S. G., and Simons-Morton, B. G. (2017). Evaluation of Risk  
286 Change-point for Novice Teenage Drivers. *Accident Analysis & Prevention*, 108:139–146.

287 Liu, Y. and Guo, F. (2019). A Bayesian Time-Varying Coefficient Model for Multitype  
 288 Recurrent Events. *Journal of Computational and Graphical Statistics*, pages 1–12.

289 Liu, Y., Guo, F., and Hanowski, R. J. (2019). Assessing the Impact of Sleep Time on Truck  
 290 Driver Performance using a Recurrent Event Model. *Statistics in Medicine*, 38(21):4096–  
 291 4111.

292 Lord, D. and Mannering, F. (2010). The Statistical Analysis of Crash-Frequency Data: A  
 293 Review and Assessment of Methodological Alternatives. *Transportation Research Part A:  
 294 Policy and Practice*, 44(5):291–305.

295 Mannering, F. L. and Bhat, C. R. (2014). Analytic Methods in Accident Research: Method-  
 296 ological Frontier and Future Directions. *Analytic Methods in Accident Research*, 1:1–22.

297 Mehdizadeh, A., Cai, M., Hu, Q., Yazdi, A., Ali, M., Mohabbati-Kalejahi, N., Vinel, A.,  
 298 Rigdon, S. E., Davis, K. C., and Megahed, F. M. (2020). A Review of Data Analytic  
 299 Applications in Road Traffic Safety. Part 1: Descriptive and Predictive Modeling. *Sensors*,  
 300 20(4):1107.

301 Rigdon, S. E. and Basu, A. P. (1989). The Power Law Process: A Model for the Reliability  
 302 of Repairable Systems. *Journal of Quality Technology*, 21(4):251–260.

303 Rigdon, S. E. and Basu, A. P. (2000). *Statistical Methods for the Reliability of Repairable  
 304 Systems*. Wiley New York.

305 Savolainen, P. T., Mannering, F. L., Lord, D., and Quddus, M. A. (2011). The Statistical  
 306 Analysis of Highway Crash-injury Severities: A Review and Assessment of Methodological  
 307 Alternatives. *Accident Analysis & Prevention*, 43(5):1666–1676.



- 308 Stan Development Team (2018). RStan: the R interface to Stan. R package version 2.18.2.
- 309 The Dark Sky Company, LLC (2020). Dark Sky API — Overview. [https://darksky.net/](https://darksky.net/dev/docs)
- 310 [dev/docs](https://darksky.net/dev/docs). [Online; accessed 20-February-2020].